JOURNAL OF PROPULSION AND POWER
Vol. 15, No. 6, November–December 1999

# Ignition Pressure Transient in Solid Rockets Initially Filled with Water

Sergey S. Bondarchuk* and Aleksander B. Vorozhtsov†
*Tomsk State University, 634050, Tomsk, Russia*
and
Nikolai A. Obukhov‡
*State Rocket Center, 456300, Miass, Chelyabinsk Region, Russia*

**A mathematical model has been developed for the ignition transient of a solid-propellant rocket motor initially filled with water. The model predicts the gradual ignition of the propellant grains, the rise in chamber pressure, the displacement of water from the motor, and the transition to the quasi-stationary conditions. The results of parametric calculations are presented that show the effect of the initial depth of rocket submergence in the water (environment pressure) and wave processes on the ignition pressure transient. The development of previous experimental and analytical studies conducted in this laboratory is extended.**

## Nomenclature

$A$ = gas-permeable surface
$C_p$ = specific heat of gas components or mixture
$c$ = mass concentration
$D$ = number of grains forming the igniter
$E_a$ = ratio of propellant activation energy to universal gas constant
$e$ = web thickness of igniter grain
$\boldsymbol{f}$ = friction stress
$H_0$ = enthalpy of combustion product
$L$ = number of gaseous components of mixture
$M$ = mass supply density
$\boldsymbol{n}$ = unit vector of external normal to surface
$\boldsymbol{P}$ = impulse flux, $p\boldsymbol{n} + \boldsymbol{u}N$
$p$ = pressure
$Q_o$ = ratio of propellant explosion heat to propellant specific heat
$q$ = heat flux density
$R$ = gas constant
$S$ = gas-impermeable surface
$T$ = propellant temperature
$T_g$ = temperature of gas
$T_p$ = isobaric combustion temperature
$t$ = time
$\boldsymbol{u}$ = velocity vector
$V$ = volume
$W$ = interior free volume of igniter device
$w$ = current volume of pyrogranules
$x$ = axial coordinate
$y$ = axis normal to propellant surface
$Z$ = preexponential factor
$z$ = portion of condensed phase in combustion products
$\alpha$ = effective heat emission coefficient, which includes radiant and convective components
$\varepsilon$ = adiabatic index (ratio of specific heats)
$\kappa$ = thermal diffusivity of solid propellant
$\lambda$ = thermal conductivity
$\rho$ = density

*Subscripts*

$e$ = external environment
$j$ = individual features of the components

Received 4 February 1998; revision received 27 November 1998; accepted for publication 27 November 1998. 

*Senior Researcher, Research and Development Department.
†Professor, Research and Development Department.
‡Head of Laboratory.

## Introduction

WHEN launching a rocket from underwater, or from the surface, conventional ignition methods easily can generate excessive pressures in the combustion chamber and in any surrounding structures. This problem is avoided by initially pressurizing the combustion chamber with inert gases from separate pressurized gas cylinders. There is another more effective method of preignition or prelaunch supercharges, using a low-temperature gas generator. However, if the combustion products have a temperature above 100°C, they may produce an unplanned ignition of the rocket motor propellant. Preliminary experiments are needed to prevent this accidental ignition.

One more way of reducing the gas charge and preventing excessive pressures is to fill the rocket motor with water. This method requires proper study because the contact between the water, the gas charge, and the propellant surface may change the propellant's ignition characteristics as a result of the propellant ingredients being leached.[1] Direct contact of seawater with the propellant surface can be excluded by using a thin protective layer.

In this study, three kinds of motors were studied numerically: 1) motors with regular launching conditions; 2) motors with preliminary gas injection; and 3) motors filled with seawater (Fig. 1). Case 3 is considered to be the most complicated. Here, the head end of the combustion chamber is fitted with an ignition system. The quantity of the volume, its geometry, and the gas parameters are defined by the external pressure. The igniter is a pressure-proof, perforated cylinder, which contains pyrogranules or charge of the solid propellant. Then, after the signal is sent, the ignition system starts producing combustion products. These products increase the pressure in the head volume and displace the water from the combustion chamber through the nozzle of the motor. The surface of the propellant charge is exposed to the high-temperature combustion products, the surface layer of the charge is heated, and the bare element of the solid propellant eventually ignites. The combination of the igniter and the propellant combustion products leads to a rapid rise in chamber pressure and water displacement When the igniter propellant is consumed and all the water is displaced, the motor transitions to the quasi-stationary conditions.

In case 2, where the blowoff is provided by compressed gas, initiation of the gas flow is considered to be the initial event. This analysis also examines the movements of the gas, e.g., the products

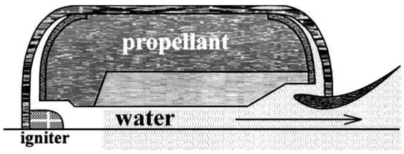


**Fig. 1 Calculation region.**

from the igniter and external gas source, through the nozzle of the rocket motor, their heat transfer to the propellant surface, and the resulting heating (or cooling) of the surface.

## Mathematical Model

The mathematical model of the processes described above is based on the integral equations of the gasdynamics derived from the laws of mass, momentum, and energy conservation. Additional special equations define the thermal and physical properties of the multicomponent combustion products from the igniter charge and the air that initially fills the chamber. This system of equations is applied to a reference volume $V$, bounded by a closed surface comprising both gas-permeable $A$ and gas-impermeable $S$ materials. Heat and mass are exchanged between gas flow and rocket-motor elements. The change in the mass, momentum, and energy in the control volume is connected through volume interactions, the influence of the external surroundings on each of the mentioned quantities, and their transfer through $A$. This system of conservation equations is written in the integral form with a generalized coordinate system[2] as follows:

$$\frac{\partial}{\partial t}\int_V \rho\,\mathrm{d}V + \int_A \rho N\,\mathrm{d}A = \int_S \sum_{j=1}^{L} M_j\,\mathrm{d}S$$

$$\frac{\partial}{\partial t}\int_V \rho R\,\mathrm{d}V + \int_A \rho R N\,\mathrm{d}A = \int_S \sum_{j=1}^{L} R_j M_j\,\mathrm{d}S$$

$$\frac{\partial}{\partial t}\int_V \rho C_p\,\mathrm{d}V + \int_A \rho C_p N\,\mathrm{d}A = \int_S \sum_{j=1}^{L} C_{p_j} M_j\,\mathrm{d}S$$

$$\frac{\partial}{\partial t}\int_V \rho \boldsymbol{u}\,\mathrm{d}V + \int_A \boldsymbol{P}\,\mathrm{d}A + \int_S \boldsymbol{P}\,\mathrm{d}S + \int_S \rho \boldsymbol{f}\,\mathrm{d}S = 0$$

$$\frac{\partial}{\partial t}\int_V E\,\mathrm{d}V + \int_A (E+p) N\,\mathrm{d}A + \int_S q\,\mathrm{d}S = \int_S \sum_{j=1}^{L} H_{0j} M_j\,\mathrm{d}S$$

where

$$N = (\boldsymbol{u}, \boldsymbol{n}), \qquad E = \frac{p}{\gamma - 1} + \frac{\rho|u|^2}{2}, \qquad \gamma = \frac{C_p}{C_p - R}$$

One of the difficult problems to be solved in parallel with predicting the gasdynamic flowfield is the surface heating and subsequent ignition of a solid-propellant surface element. It is assumed that the ignition of the surface element occurs instantaneously when the surface temperature reaches a certain value, at which point the heat flux to the propellant surface generated by the propellant combustion products becomes larger than the heat flux from the ignition system. In other words, the ignition time is based on the condensed-phase ignition model developed by Vilyunov and Zarko[3] and other authors. Mathematically, this model of ignition of a condensed substance (solid propellant) involves the transient equation for thermal conductivity, which also takes into account the heat release term and chemical kinetics:

$$\frac{\partial T}{\partial t} = \alpha \frac{\partial^2 T}{\partial x^2} + Q_o \cdot F(c, T), \qquad \frac{\partial T}{\partial t} = -F(c, T)$$

$$F(c, T) = Zc \cdot \exp(-E_a/T)/\rho_o$$

Here, the rate of the chemical reactions is characterized by the Arrhenius relation. The effect of hot gaseous combustion products on the charge is simulated by establishing the boundary conditions of the third kind at the solid-propellant surface and by setting the heat flux at infinity to be zero:

$x = 0$:

$$\alpha[T_g - T(0, t)] = -\lambda \frac{\partial T}{\partial x}$$

$x = \infty$:

$$-\lambda \frac{\partial T}{\partial x} = 0$$

The thermodynamics of the gas mixture in the igniter (indestructible perforated casing) is described by averaged parameters. In this case, the mathematical model describing the variation of gasdynamic parameters in the volume of the igniter casing is a system of lumped or nondimensional differential equations for interior free volume $W$. It also is assumed that the entire surface $D$ of the igniter grains is ignited instantaneously and that the perforated casing prevents the escape of these grains.

The system of equations for the conservation of mass and energy and for variation in the free interior volume in the igniter then becomes

$$\frac{\mathrm{d}}{\mathrm{d}t}(\rho W) = \sum_{i=1}^{D}(1 - z_i) M_i - M_*$$

$$\frac{\mathrm{d}}{\mathrm{d}t}(\rho R W) = \sum_{i=1}^{D}(1 - z_i) R_i M_i - R M_*$$

$$\frac{\mathrm{d}}{\mathrm{d}t}(\rho C_p W) = \sum_{i=1}^{D}(1 - z_i)(C_p)_i M_i - C_p M_*$$

$$\frac{\mathrm{d}}{\mathrm{d}t}\left(\frac{pW}{\gamma - 1}\right) = \sum_{i=1}^{D}(1 - z_i)(C_p)_i (T_p)_i M_i - \frac{\gamma}{\gamma - 1}\frac{p}{\rho} M_*$$

$$\frac{\mathrm{d}W}{\mathrm{d}t} = -\sum^{D}_{i=1} \frac{\mathrm{d}\omega}{\mathrm{d}t}$$

The gas flow $M_*$ through the perforation holes is calculated by the familiar quasi-stationary equations

$$M_* = S_p \begin{cases} \sqrt{\gamma m^{(\gamma+1)/(\gamma-1)} p\rho}, & \psi \le m^n \\ \sqrt{2np\rho(\psi^{2/\gamma} - \psi^{1/n})}, & m^n < \psi < 1 \\ 0, & \psi \ge 1 \end{cases}$$

where $S_p$ is gas-permeable surface of igniter box

$$n = \frac{\gamma}{\gamma - 1}, \qquad m = \frac{2}{\gamma + 1}, \qquad \psi = \frac{p_k}{p}$$

where $p_k$ is external (in the chamber) pressure.

The mass flow rate of gas is related to the change in the volume $\omega$ of burning igniter material as follows:

$$M_i = -(\rho_o)_i \frac{\mathrm{d}\omega_i}{\mathrm{d}t}, \qquad i = 1, \ldots, D$$

The instantaneous volume of the pyrotechnic grains depends on the flame depth ($m_o/\rho_o \ge \omega \ge 0$, $m_o$, $\rho_o$—mass and density) and is a function of the grain shape. For a wide spectrum of shapes, the relationship between the instantaneous volume of these grains $\varpi$ and their sizes is very simple:

$$\omega_i = \frac{(m_o)_i}{(\rho_o)_i} \frac{\prod_{j=1}^{3}(e_{ij} - e_i)}{\prod_{j=1}^{3} e_{ij}}$$

where $e_{ij}$ ($j = 1, 2, 3$) are the initial geometric characteristic features of the $i$ grain.

The variation of typical sizes of a grain as a result of burning is described through the burn depth $e_i$ as defined by the equation

$$\frac{\mathrm{d}e_i}{\mathrm{d}t} = r_i$$

$i = 1, \ldots, D$ where $r$ is burning rate. The motion of the boundary between gas and water inside the motor is coupled to the motion of the water through the nozzle area $S_*$. The water flow rate through the nozzle is determined by the difference between the instantaneous gas pressure and the exterior water pressure by use of the following formula:

$$\frac{\partial}{\partial t}\int_V \mathrm{d}V = S_*\sqrt{\frac{2}{\rho}(p - p_e)}$$

These equations of motion were integrated by a second-order modification to the method developed by Godunov.[4] The mathematical problem in the ignition of a solid propellant was solved using an adaptable calculation grid that varied with the heating condition.[5]

## Results of Calculations

The numerical comparative analysis of local and integral parameters of the physical processes were made for a motor with the following general characteristics: 3 m long, 16-m$^2$ propellant surface area; 2.2 m motor diameter; 0.16-m nozzle throat diameter. The propellant's combustion temperature was assumed to be 3340 K. The igniter combustion products weighed 2.5 kg, contained up to 50% of condensed-phase material and had a temperature of 3320 K.

For comparative analysis, the following three sets of the motor startup conditions were considered:

1) starting at nominal initial conditions of $T = 293$ K and $p = 0.1$ MPa and with nozzle membrane burst of 1 MPa,

2) starting the motor after pressurizing with a gas generator producing $G = 50$ kg/s of gas without metal at 400 K,

3) starting after filling the motor with water.

Cases 2 and 3 were examined for external pressures over the range of 0.5, 1.0, 1.5, and 2.0 MPa. In case 2, the gas generator was assumed to pressurize the combustion chamber to the external pressure, at which time the gas generator stopped working, the igniter switched on, and a new time reading started.

Figure 2 gives the chamber pressure and motor thrust dependence during startup under normal conditions. In the initial time after actuating the igniter, the chamber pressure increase reaches the bursting pressure of the nozzle membrane and it bursts. Rarefaction waves pass along the channel of the charge (Figs. 3 and 4, $t \approx 0.018$ s). At time $t \approx 0.015$ s, ignition of the charge starts from the head end (see Fig. 5), producing considerable inhomogeneity in the heating, which lasts for about 0.0065 s (from $t \approx 0.015$ to 0.0215 s). The pressure in the combustion chamber begins to rise sharply (see Fig. 2, $t > 0.021$ s) and, after complete combustion of the igniter, the motor transitions to the steady-state regime. The curve of changing thrust

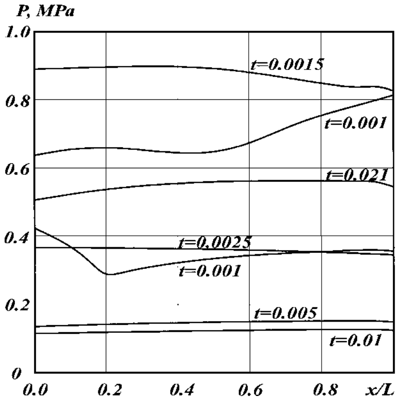


Fig. 3 Pressure distribution.

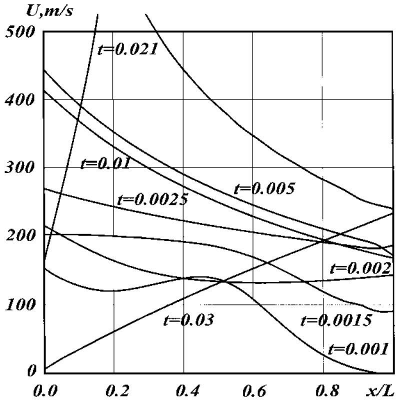


Fig. 4 Velocity distribution.

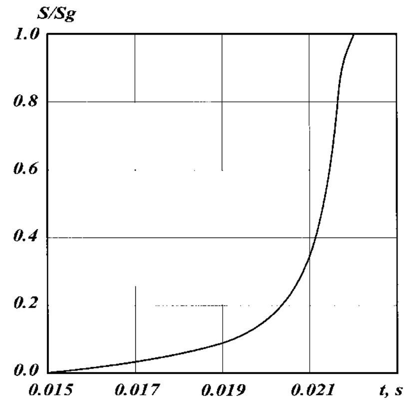


Fig. 5 Combustion surface.

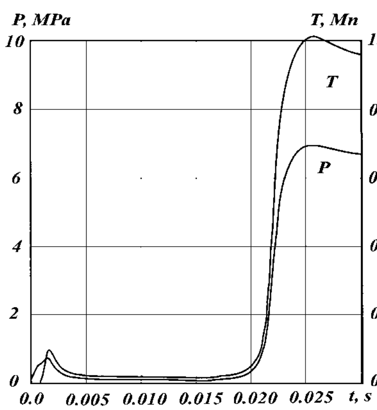


Fig. 2 Pressure and thrust dependencies under normal condition.

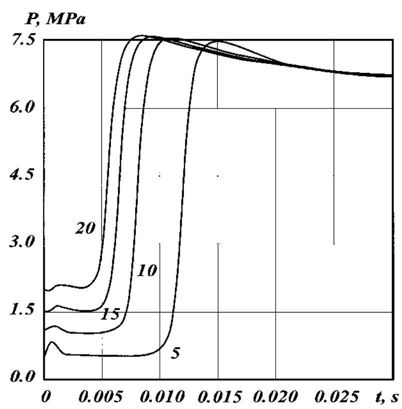


Fig. 6 Pressure dependencies.

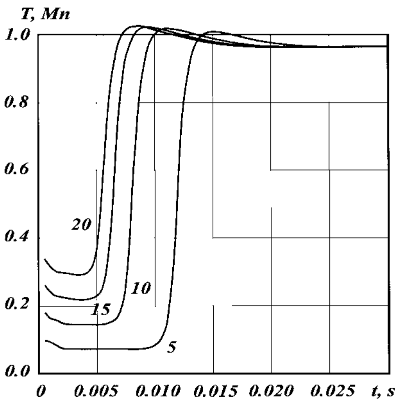


Fig. 7 Thrust dependencies.

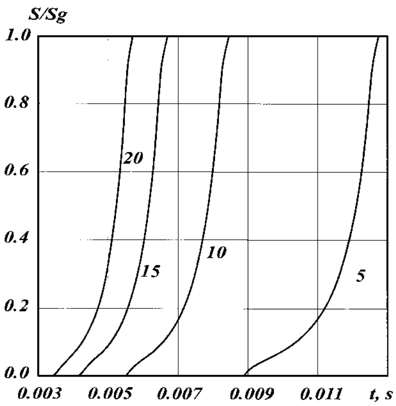


Fig. 8 Combustion surface.

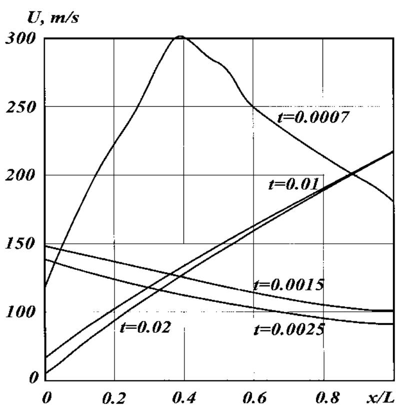


Fig. 9 Velocity distribution.

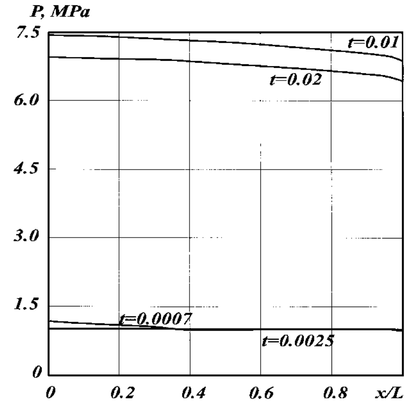


Fig. 10 Pressure distribution.

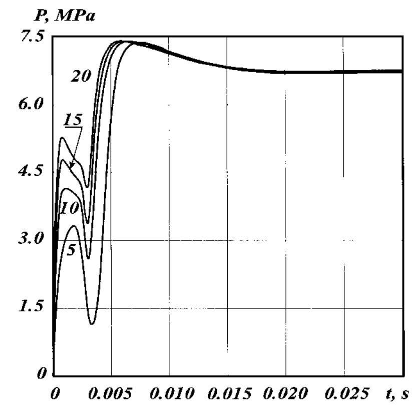


Fig. 11 Pressure dependencies.

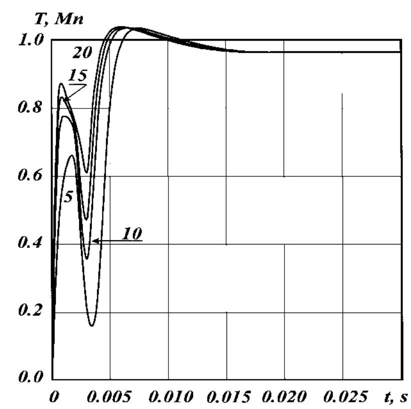


Fig. 12 Thrust dependencies.

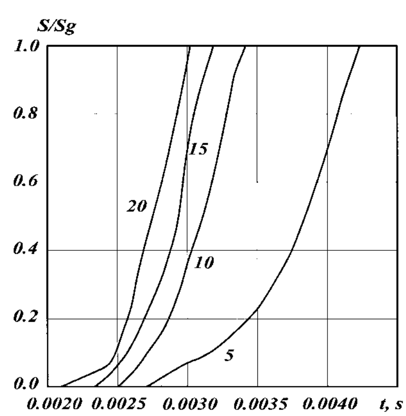


Fig. 13 Combustion surface.

follows the change of pressure in the cavity of the motor, as illustrated in Fig. 2. The pattern of the wave processes accompanying startup of the motor and the changes in the spacial distributions of gasdynamic parameters are given in Figs. 3 and 4.

Figure 6 shows the effect of environmental pressure on the chamber pressure transient and Fig. 7 shows the corresponding motor thrust transient for environmental pressures of 0.5, 1.0, and 2.0 MPa. Analysis of the results shows that, as expected, motors with higher levels of initial pressure come to the steady-state regime more rapidly. This behavior is expected because the heating rate of the charge by the combustion products of a gas generator before starting up the motor is higher for higher levels of the supercharge pressure producing shorter periods of ignition time. Ignition of the charge after actuating the igniter starts considerably earlier (at the level of $t \approx 0.008$ s) and occurs approximately 2 times faster than starting under normal conditions. Figure 8 shows the time pattern of the charge's burning surface for the various levels of environmental

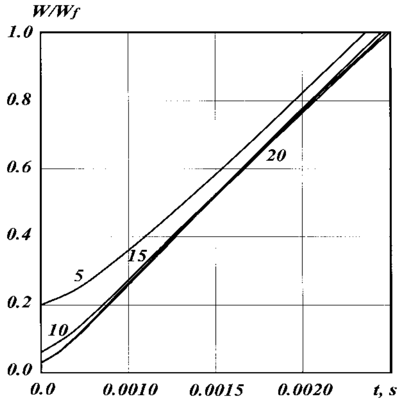


**Fig. 14 Free volume dependence.**

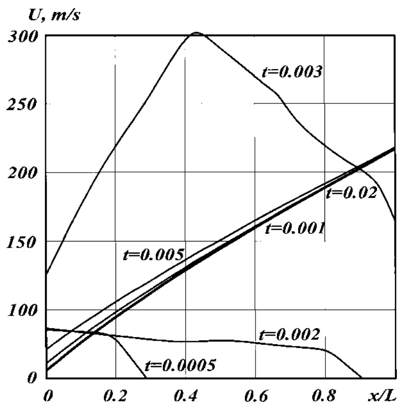


**Fig. 15 Velocity distribution.**

pressure. Figures 9 and 10 show the spatial distributions of gasdynamic parameters for 1 MPa at different moments of time. As a whole, the wave processes are markedly weaker than when starting under normal conditions, as expected.

Analyses of igniting motors with their chamber initially filled with water is illustrated in Figs. 11–16. Figure 11 shows the pressure transient and Fig. 12 shows the corresponding thrust transient for different external pressures. The fundamental difference produced by the water is the rather high level of the motor thrust at the initial moments of igniter operation, caused by water displacement because its density is several orders higher than the gas density. For all of the conditions studied, the following pattern characterizes the evolution of the ignition process. The igniter starts working at the high initial pressure over a small free volume. As a result, the gas pressure and temperature increase sharply. Simultaneously with a gradual displacement of the fluid, the charge surface is exposed to intensive heating and propellant ignition starts almost immediately (in the case of an external pressure 2.0 MPa, it is even a little earlier) after displacing the water ($t \approx 0.0023 \div 0.0025$ s). Accordingly, the initial pressure in the combustion chamber can somewhat exceed the steady-state value that is achieved after complete combustion of an igniter. Figure 13 shows the time evolution of the

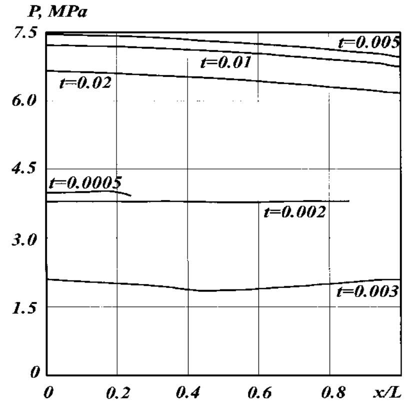


**Fig. 16 Pressure distribution.**

charge's burning surface. The time of initial ignition and the time to ignite the surface completely for these conditions is slightly less ($\Delta t \approx 0.001$ s) than in the case of starting the motor after preliminary gas pressurization.

In Fig. 14, the time dependencies of changing motor free volume during the startup period are given. It is seen that higher levels of external pressure require more time to fill the chamber, though, the differences are generally insignificant. Figures 15 and 16 illustrate the spatial distribution of the gas velocity and pressure at different times for an external pressure of 1 MPa. The characteristics of the wave processes during the motor's transition to the steady-state regime are slightly softened because of the moving surface of the displaced liquid.

## Conclusions

A physicomathematical model is used to analyze the ignition characteristics of starting solid-propellant motors initially filled with water. Analysis of the calculations shows that the water produces fundamental peculiarities in the speed of flame propagation over the propellant surface, the growth rate of the chamber pressure, and the character of motor's thrust transient. It is shown that the time to achieve steady-state operation is considerably less than when the motor is pressurized by a gas generator and when ignition occurs under normal conditions.

## References

[1]Velichko, I. I., Obukhov, N. A., and Shishkin, V. S., "Fresh Approach to Solid Rocket Motor Design," *Journal of Propulsion and Power*, Vol. 11, No. 4, 1995, pp. 579–582.

[2]Bondarchuk, S. S., Vorozhtsov, A. B., Kozlov, E. A., and Feshenko, Y. V., "Analysis of Multidimensional and Two-Phase Flows in Solid Rocket Motors," *Journal of Propulsion and Power,* Vol. 11, No. 4, 1995, pp. 593–599.

[3]Vilyunov, V. N., and Zarko, V. E., *Ignition of Solids*, Elsevier, Amsterdam, 1989, p. 441.

[4]Godunov, S. K., Zabrodin, A. U., Ivanov, M. Y., Kraiko, A. N., and Prokopov, G. P., *Numerical Solution of Multidimensional Problems of Gas Dynamics*, Nauka, Moscow, 1982, p. 400.

[5]Borovskoy, I. G., Bondarchuk, S. S., Kozlov, E. A., and Vilunov, V. N., "Solution of the Problem of Condensed System Ignition Based on a Difference Scheme with Time-Dependent Grid," *Fizika Gorenia i Vzryva*, Vol. 22, No. 3, 1986, pp. 14–19.